Eur. Phys. J. Plus (2016) **131**: 356
DOI 10.1140/epjp/i2016-16356-3

THE EUROPEAN PHYSICAL JOURNAL PLUS

Regular Article

Numerical simulation for treatment of dispersive shallow water waves with Rosenau-KdV equation

Turgut Ak[1,a], S. Battal Gazi Karakoc[2], and Houria Triki[3]

[1] Faculty of Engineering, Department of Transportation Engineering, Yalova University, 77100 Yalova, Turkey
[2] Faculty of Science and Art, Department of Mathematics, Nevsehir Haci Bektas Veli University, 50300 Nevsehir, Turkey
[3] Radiation Physics Laboratory, Department of Physics, Faculty of Sciences, Badji Mokhtar University, P.O. Box 12, 23000 Annaba, Algeria

Received: 23 May 2016 / Revised: 29 August 2016
Published online: 12 October 2016 –

Abstract. In this paper, numerical solutions for the Rosenau-Korteweg-de Vries equation are studied by using the subdomain method based on the sextic B-spline basis functions. Numerical results for five test problems including the motion of single solitary wave, interaction of two and three well-separated solitary waves of different amplitudes, evolution of solitons with Gaussian and undular bore initial conditions are obtained. Stability and *a priori* error estimate of the scheme are discussed. A comparison of the values of the obtained invariants and error norms for single solitary wave with earlier results is also made. The results show that the present method is efficient and reliable.

1 Introduction

Interest in travelling-wave solutions for nonlinear partial differential equations (NLPDEs) has grown rapidly in recent years because of their importance in the study of complex nonlinear phenomena arising in dynamical systems. Such nonlinear wave phenomena appear in various fields of sciences, particularly in fluid mechanics, solid state physics, plasma physics and nonlinear optics.

A variety of powerful methods have been developed to find analytical and numerical solutions of NLPDEs of all kinds. Examples include the Petrov-Galerkin method [1], the collocation method [2], the subsidiary ordinary differential equation method [3–5], Hirota's method [6], the solitary wave ansatz method [7,8], Exp-function method [9], and many others.

The well-known Korteweg-de Vries (KdV) equation [10]

$$U_t + aUU_x + bU_{xxx} = 0, \tag{1}$$

where U is a real-valued function and a and b are real constants, is the generic model for the study of weakly nonlinear long waves [11]. It arises in physical systems which involve a balance between nonlinearity and dispersion at leading-order [12]. For example, it describes surface waves of long wavelength and small amplitude on shallow water and internal waves in a shallow density-stratified fluid [12].

In 1988, Philip Rosenau [13] introduced the Rosenau equation of the form

$$U_t + \kappa U_x + cU_{xxxxt} + d\left(U^2\right)_x = 0, \tag{2}$$

to describe the dynamics of dense discrete systems.

For further consideration of the nonlinear wave, Zuo [14] added the viscous term U_{xxx} to the Rosenau equation (2) and proposed the so-called Rosenau-KdV equation. The author obtained some solitons and periodic wave solutions of

[a] e-mail: akturgut@yahoo.com

model combining the original KdV equation and Rosenau equation by means of the sine-cosine and the tanh methods. This physically interesting model reads

$$U_t + aU_x + bU_{xxx} + cU_{xxxxt} + d\left(U^2\right)_x = 0. \tag{3}$$

Here in (3), the dependent variable $U(x,t)$ represents the shallow water wave profile while the independent variables x and t represent the spatial and temporal variables, respectively. The coefficient of a represents the drifting term, the coefficient of b is the third-order dispersion and the coefficient of c represents the higher-order dispersion term. Finally, the last term with d is the nonlinear term.

In ref. [15] the sech-ansatz method was applied to obtain explicit solitary wave solutions for the generalized Rosenau-KdV equation with power law nonlinearity parameter. Besides, the exact topological 1-soliton solution of the generalized Rosenau-KdV equation has been recently obtained by using the solitary wave ansatz method [16]. The singular 1-soliton solution of Rosenau-KdV equation is derived by the ansatz method. Subsequently, the soliton perturbation theory is applied to obtain the adiabatic parameter dynamics of the water waves. Finally, the integration of the perturbed Rosenau-KdV equation is obtained by the ansatz method as well as the semi-inverse variational principle [17]. A conservative three-level lineer finite difference scheme (CLDS) for the numerical solution of the initial-boundary value problem of Rosenau-KdV equation is proposed. It is shown that the finite difference scheme is of second order convergence and unconditionally stable [18]. A mathematical model to obtain the solution of the nonlinear wave by coupling the Rosenau-KdV equation and the Rosenau-RLW equation is suggested. A numerical tool is applied to the model by using a three-level average implicit finite difference technique [19]. An average linear finite difference scheme for the numerical solution of the initial boundary value problem of the generalized Rosenau-KdV equation is presented. The existence, uniqueness, and conservation for energy of the difference solution are proved by the discrete energy norm method [20]. The collocation finite element method (CFEM) is utilized to simulate the motion of single solitary wave with Rosenau-KdV equation. Applying the von-Neumann stability analysis, the proposed method is illustrated to be unconditionally stable [21].

In the present paper, we use a numerical scheme based on the sextic B-spline basis functions to solve the Rosenau-KdV equation. The method is tested on five problems including the motion of single solitary wave, interaction of two and three solitary waves, evolution of solitons with Gaussian and undular bore initial conditions.

The paper is organized as follows: B-Spline basis functions used to construct numerical solutions to the Rosenau-KdV equation are described in sect. 2. The application of subdomain method to the governing wave equation is presented in sect. 3. The stability of the scheme is proved in sect. 4. Numerical results for the motion and interaction of solitary wave are reported in sect. 5. Evolution of a train of solitons for the present model is also studied using the Gaussian and undular bore initial conditions. Finally, we summarize our findings in sect. 6.

2 The governing equation and sextic B-spline basis functions

In this study, we will consider the Rosenau-Korteweg-de Vries (R-KdV) equation

$$U_t + aU_x + bU_{xxx} + cU_{xxxxt} + d\left(U^2\right)_x = 0, \tag{4}$$

with the physical boundary conditions $U \to 0$ as $x \to \pm\infty$, where a, b, c and d are positive parameters and the subscripts x and t denote the differentiation. To implement the numerical method, solution domain is restricted over an interval $a \le x \le b$. Boundary conditions will be selected from the following homogeneous boundary conditions:

$$\begin{aligned} &U(a,t) = 0, \qquad U(b,t) = 0, \\ &U_x(a,t) = 0, \qquad U_x(b,t) = 0, \\ &U_{xx}(a,t) = 0, \qquad U_{xx}(b,t) = 0, \quad t > 0, \end{aligned} \tag{5}$$

and the initial condition

$$U(x,0) = f(x), \quad a \le x \le b. \tag{6}$$

Table 1. Sextic B-spline function and its derivatives at nodes x_m.

x	x_{m-3}	x_{m-2}	x_{m-1}	x_m	x_{m+1}	x_{m+2}	x_{m+3}
$\phi_m(x)$	1	57	302	302	57	1	0
$h\phi'_m(x)$	-6	-150	-240	240	150	6	0
$h^2\phi''_m(x)$	30	270	-300	-300	270	30	0
$h^3\phi'''_m(x)$	-120	-120	960	-960	120	120	0
$h^4\phi^{iv}_m(x)$	360	-1080	720	720	-1080	360	0
$h^5\phi^{v}_m(x)$	-720	3600	-7200	7200	-3600	720	0

The sextic B-splines $\phi_m(x)$, $(m = -3(1)N + 2)$, at the knots x_m are defined over the interval $[a, b]$ by the relationships ref. [22]

$$\phi_m(x) = \frac{1}{h^6}\begin{cases} (x - x_{m-3})^6, & x \in [x_{m-3}, x_{m-2}], \\ (x - x_{m-3})^6 - 7(x - x_{m-2})^6, & x \in [x_{m-2}, x_{m-1}], \\ (x - x_{m-3})^6 - 7(x - x_{m-2})^6 + 21(x - x_{m-1})^6, & x \in [x_{m-1}, x_m], \\ (x - x_{m-3})^6 - 7(x - x_{m-2})^6 + 21(x - x_{m-1})^6 - 35(x - x_m)^6, & x \in [x_m, x_{m+1}], \\ (x - x_{m+4})^6 - 7(x - x_{m+3})^6 + 21(x - x_{m+2})^6, & x \in [x_{m+1}, x_{m+2}], \\ (x - x_{m+4})^6 - 7(x - x_{m+3})^6, & x \in [x_{m+2}, x_{m+3}], \\ (x - x_{m+4})^6, & x \in [x_{m+3}, x_{m+4}], \\ 0, & \text{otherwise.} \end{cases} \tag{7}$$

The set of functions $\{\phi_{-3}(x), \phi_{-2}(x), \phi_{-1}(x), \phi_0(x), \ldots, \phi_{N+1}(x), \phi_{N+2}(x)\}$ forms a basis for approximate solution defined over $[a, b]$. The approximate solution $U_N(x, t)$ to the exact solution $U(x, t)$ is given by

$$U_N(x, t) = \sum_{i=-3}^{N+2} \phi_i(x)\delta_i(t), \tag{8}$$

where $\delta_i(t)$ are time-dependent parameters to be determined from the boundary and subdomain conditions. Each sextic B-spline covers seven elements so that each element $[x_m, x_{m+1}]$ is covered by seven splines. The values of $\phi_m(x)$ and its derivative may be tabulated as in table 1.

Using trial function (8) and sextic B-splines (7), the values of U, U', U'', U''', U^{iv} and U^v at the knots are determined in terms of the element parameters δ_m by

$$\begin{aligned} U_m &= U(x_m) = \delta_{m-3} + 57\delta_{m-2} + 302\delta_{m-1} + 302\delta_m + 57\delta_{m+1} + \delta_{m+2}, \\ U'_m &= U'(x_m) = \frac{6}{h}(-\delta_{m-3} - 25\delta_{m-2} - 40\delta_{m-1} + 40\delta_m + 25\delta_{m+1} + \delta_{m+2}), \\ U''_m &= U''(x_m) = \frac{30}{h^2}(\delta_{m-3} + 9\delta_{m-2} - 10\delta_{m-1} - 10\delta_m + 9\delta_{m+1} + \delta_{m+2}), \\ U'''_m &= U'''(x_m) = \frac{120}{h^3}(-\delta_{m-3} - \delta_{m-2} + 8\delta_{m-1} - 8\delta_m + \delta_{m+1} + \delta_{m+2}), \\ U^{iv}_m &= U^{iv}(x_m) = \frac{360}{h^4}(\delta_{m-3} - 3\delta_{m-2} + 2\delta_{m-1} + 2\delta_m - 3\delta_{m+1} + \delta_{m+2}), \\ U^{v}_m &= U^{v}(x_m) = \frac{720}{h^5}(-\delta_{m-3} + 5\delta_{m-2} - 10\delta_{m-1} + 10\delta_m - 5\delta_{m+1} + \delta_{m+2}), \end{aligned} \tag{9}$$

where the symbols $'$, $''$, $'''$, ^{iv} and ^{v} denote differentiation with respect to x.

A typical finite interval $[x_m, x_{m+1}]$ is turned into the interval $[0, 1]$ by local coordinates ξ regarding the global coordinates

$$h\xi = x - x_m, \quad 0 \le \xi \le 1, \tag{10}$$

so the sextic B-spline shape functions over the element $[0,1]$ can be defined as $\phi^e = (\phi_{m-3}, \phi_{m-2}, \phi_{m-1}, \phi_m, \phi_{m+1}, \phi_{m+2}, \phi_{m+3})$,

$$\phi^e = \begin{cases} \phi_{m-3} = 1 - 6\xi + 15\xi^2 - 20\xi^3 + 15\xi^4 - 6\xi^5 + \xi^6, \\ \phi_{m-2} = 57 - 150\xi + 135\xi^2 - 20\xi^3 - 45\xi^4 + 30\xi^5 - 6\xi^6, \\ \phi_{m-1} = 302 - 240\xi - 150\xi^2 + 160\xi^3 + 30\xi^4 - 60\xi^5 + 15\xi^6, \\ \phi_m = 302 + 240\xi - 150\xi^2 - 160\xi^3 + 30\xi^4 + 60\xi^5 - 20\xi^6, \\ \phi_{m+1} = 57 + 150\xi + 135\xi^2 + 20\xi^3 - 45\xi^4 - 30\xi^5 + 156\xi^6, \\ \phi_{m+2} = 1 + 6\xi + 15\xi^2 + 20\xi^3 + 15\xi^4 + 6\xi^5 - 6\xi^6, \\ \phi_{m+3} = \xi^6. \end{cases} \tag{11}$$

All spline functions apart from $\phi_{m-3}(x)$, $\phi_{m-2}(x)$, $\phi_{m-1}(x)$, $\phi_m(x)$, $\phi_{m+1}(x)$, $\phi_{m+2}(x)$, $\phi_{m+3}(x)$ are zero over the element $[0,1]$. Approximation (8) over this element can be noted down in terms of basis functions (11) as

$$U_N(\xi, t) = \sum_{i=m-3}^{m+3} \delta_i(t)\phi_i(\xi), \tag{12}$$

where δ_{m-3}, δ_{m-2}, δ_{m-1}, δ_m, δ_{m+1}, δ_{m+2}, δ_{m+3} act as element parameters and B-splines $\phi_{m-3}(x)$, $\phi_{m-2}(x)$, $\phi_{m-1}(x)$, $\phi_m(x)$, $\phi_{m+1}(x)$, $\phi_{m+2}(x)$ and $\phi_{m+3}(x)$ as element shape functions. Application of subdomain method to eq. (3) with weight function

$$W_m(x) = \begin{cases} 1, & x \in [x_m, x_{m+1}], \\ 0, & \text{otherwise}, \end{cases} \tag{13}$$

creates the weak form

$$\int_{x_m}^{x_{m+1}} 1 \cdot \left[U_t + aU_x + bU_{xxx} + cU_{xxxxt} + d\left(U^2\right)_x\right] \mathrm{d}x = 0. \tag{14}$$

3 Subdomain finite element method

Substituting the transformation (11) into weak form (14) and integrating eq. (14) term by term with some manipulation by parts, gives

$$\begin{aligned} &\frac{h}{7}(\dot{\delta}_{m-3} + 120\dot{\delta}_{m-2} + 1191\dot{\delta}_{m-1} + 2416\dot{\delta}_m + 1191\dot{\delta}_{m+1} + 120\dot{\delta}_{m+2} + \dot{\delta}_{m+3}) \\ &+ a(-\delta_{m-3} - 56\delta_{m-2} - 245\delta_{m-1} + 245\delta_{m+1} + 56\delta_{m+2} + \delta_{m+3}) \\ &+ \frac{30b}{h^2}(-\delta_{m-3} - 8\delta_{m-2} + 19\delta_{m-1} - 19\delta_{m+1} + 8\delta_{m+2} + \delta_{m+3}) \\ &+ \frac{120c}{h^3}(\dot{\delta}_{m-3} - 9\dot{\delta}_{m-1} + 16\dot{\delta}_m - 9\dot{\delta}_{m+1} + \dot{\delta}_{m+3}) \\ &+ 2dZ_m(-\delta_{m-3} - 56\delta_{m-2} - 245\delta_{m-1} + 245\delta_{m+1} + 56\delta_{m+2} + \delta_{m+3}) = 0, \end{aligned} \tag{15}$$

where the dot indicates differentiation with respect to t and

$$Z_m = \delta_{m-3} + 57\delta_{m-2} + 302\delta_{m-1} + 302\delta_m + 57\delta_{m+1} + \delta_{m+2}. \tag{16}$$

If time parameters δ_m and its time derivatives $\dot{\delta}_m$ in eq. (15) are discretized by the Crank-Nicolson and forward difference approach respectively,

$$\delta_m = \frac{\delta_m^{n+1} + \delta_m^n}{2}, \qquad \dot{\delta}_m = \frac{\delta_m^{n+1} - \delta_m^n}{\Delta t}, \tag{17}$$

we obtain a recurrence relationship between two time levels n and $n+1$ relating two unknown parameters δ_i^{n+1}, δ_i^n, $i = m-3, m-2, \ldots, m+3$,

$$\begin{aligned} &\alpha_{m1}\delta_{m-3}^{n+1} + \alpha_{m2}\delta_{m-2}^{n+1} + \alpha_{m3}\delta_{m-1}^{n+1} + \alpha_{m4}\delta_m^{n+1} + \alpha_{m5}\delta_{m+1}^{n+1} + \alpha_{m6}\delta_{m+2}^{n+1} + \alpha_{m7}\delta_{m+3}^{n+1} \\ &= \alpha_{m7}\delta_{m-3}^n + \alpha_{m6}\delta_{m-2}^n + \alpha_{m5}\delta_{m-1}^n + \alpha_{m4}\delta_m^n + \alpha_{m3}\delta_{m+1}^n + \alpha_{m2}\delta_{m+2}^n + \alpha_{m1}\delta_{m+3}^n, \end{aligned} \tag{18}$$

where

$$\begin{aligned}
\alpha_{m1} &= 1 - E(a + dZ_m) - M + K,\\
\alpha_{m2} &= 120 - 56E(a + dZ_m) - 8M,\\
\alpha_{m3} &= 1191 - 245E(a + dZ_m) + 19M - 9K,\\
\alpha_{m4} &= 2416 + 16K,\\
\alpha_{m5} &= 1191 + 245E(a + dZ_m) - 19M - 9K,\\
\alpha_{m6} &= 120 + 56E(a + dZ_m) + 8M,\\
\alpha_{m7} &= 1 + E(a + dZ_m) + M + K,\\
m &= 0, 1, \ldots, N - 1,
\end{aligned} \tag{19}$$

and

$$E = \frac{7\Delta t}{2h}, \qquad M = \frac{105b\Delta t}{h^3}, \qquad K = \frac{840c}{h^4}. \tag{20}$$

The system (18) consists of N linear equation in $N + 6$ unknowns $(\delta_{-3}, \delta_{-2}, \ldots, \delta_{N+1}, \delta_{N+2})$. To get a solution of this system, we need six additional constraints. These are obtained from the boundary conditions (7). These conditions provide us with the elimination of the parameters δ_{-3}, δ_{-2}, δ_{-1}, δ_N, δ_{N+1} and δ_{N+2} from the system (18) which then becomes a matrix equation for the N unknowns $d = (\delta_0, \delta_1, \ldots, \delta_{N-1})$ of the form

$$A\delta^{n+1} = B\delta^n. \tag{21}$$

A lumped value for Z_m is obtained from $(U_m + U_{m+1})/2$ as

$$Z_m = \frac{1}{2}(\delta^n_{m-3} + 58\delta^n_{m-2} + 359\delta_{m-1} + 604\delta^n_m + 359\delta^n_{m+1} + 58\delta^n_{m+2} + \delta^n_{m+3}). \tag{22}$$

The resulting system can be effectively solved with a variant of the Thomas algorithm, and we need an inner iteration $\delta^{n*} = \delta^n + \frac{1}{2}(\delta^n - \delta^{n-1})$ at each time step to cope with the nonlinear term Z_m. A typical member of the matrix system (18) can be written in terms of the nodal parameters δ^n_m as

$$\begin{aligned}
&\gamma_1\delta^{n+1}_{m-3} + \gamma_2\delta^{n+1}_{m-2} + \gamma_3\delta^{n+1}_{m-1} + \gamma_4\delta^{n+1}_m + \gamma_5\delta^{n+1}_{m+1} + \gamma_6\delta^{n+1}_{m+2} + \gamma_7\delta^{n+1}_{m+3}\\
&= \gamma_7\delta^n_{m-3} + \gamma_6\delta^n_{m-2} + \gamma_5\delta^n_{m-1} + \gamma_4\delta^n_m + \gamma_3\delta^n_{m+1} + \gamma_2\delta^n_{m+2} + \gamma_1\delta^n_{m+3},
\end{aligned} \tag{23}$$

where

$$\begin{aligned}
\gamma_1 &= \alpha - \beta - \lambda + \mu,\\
\gamma_2 &= 120\alpha - 56\beta - 8\lambda,\\
\gamma_3 &= 1191\alpha - 245\beta + 19\lambda - 9\mu,\\
\gamma_4 &= 2416\alpha + 16\mu,\\
\gamma_5 &= 1191\alpha + 245\beta - 19\lambda - 9\mu,\\
\gamma_6 &= 120\alpha + 56\beta + 8\lambda,\\
\gamma_7 &= \alpha + \beta + \lambda + \mu,
\end{aligned} \tag{24}$$

and

$$\alpha = 1, \quad \beta = E(a + dZ_m), \quad \lambda = M, \quad \mu = K, \quad m = 0, 1, \ldots, N - 1. \tag{25}$$

To start the iteration relation system, eq. (17), the initial parameters must be determined by the aid of the initial condition and six boundary conditions as follows:

$$\begin{aligned}
U_N(x_m, 0) &= U(x_m, 0) = \delta^0_{m-3} + 57\delta^0_{m-2} + 302\delta^0_{m-1} + 302\delta^0_m + 57\delta^0_{m+1} + \delta^0_{m+2},\\
U'_N(a, 0) &= -\delta^0_{-3} - 25\delta^0_{-2} - 40\delta^0_{-1} + 40\delta^0_0 + 25\delta^0_1 + \delta^0_2 = 0,\\
U''_N(a, 0) &= \delta^0_{-3} + 9\delta^0_{-2} - 10\delta^0_{-1} - 10\delta^0_0 + 9\delta^0_1 + \delta^0_2 = 0,\\
U'''_N(a, 0) &= -\delta^0_{-3} - \delta^0_{-2} + 8\delta^0_{-1} - 8\delta^0_0 + \delta^0_1 + \delta^0_2 = 0,\\
U'_N(b, 0) &= -\delta^0_{N-3} - 25\delta^0_{N-2} - 40\delta^0_{N-1} + 40\delta^0_N + 25\delta^0_{N+1} + \delta^0_{N+2} = 0,\\
U''_N(b, 0) &= \delta^0_{N-3} + 9\delta^0_{N-2} - 10\delta^0_{N-1} - 10\delta^0_N + 9\delta^0_{N+1} + \delta^0_{N+2} = 0,\\
U'''_N(b, 0) &= -\delta^0_{N-3} - \delta^0_{N-2} + 8\delta^0_{N-1} - 8\delta^0_N + \delta^0_{N+1} + \delta^0_{N+2} = 0.
\end{aligned} \tag{26}$$

Eliminating δ^0_{-3}, δ^0_{-2}, δ^0_{-1}, δ^0_N, δ^0_{N+1}, δ^0_{N+2} from the system (18) we get a $N \times N$ matrix system of the form

$$W\delta^0 = B, \tag{27}$$

where W is

$$W = \begin{bmatrix} 384 & 312 & 24 & & & & & & & & \\ \frac{2681}{9} & 358 & \frac{568}{9} & 1 & & & & & & & \\ \frac{512}{9} & 303 & \frac{2719}{9} & 57 & 1 & & & & & & \\ & 1 & 57 & 302 & 302 & 57 & 1 & & & & \\ & & & & & & & 1 & 57 & \frac{2719}{9} & 303 & \frac{512}{9} \\ & & & & & & & & 1 & \frac{568}{9} & 358 & \frac{2681}{9} \\ & & & & & & & & & 24 & 312 & 384 \end{bmatrix}, \tag{28}$$

$\delta^0 = [\delta^0_0, \delta^0_1, \ldots, \delta^0_{N-1}]^T$ and $B = [U(x_0, 0), U(x_1, 0), \ldots, U(x_{N-1}, 0)]^T$. This matrix system can be solved effectively by using a variant of Thomas algorithm.

4 Stability analysis

The stability analysis is based on the von Neumann theory. The growth factor ξ of the error in a typical mode of amplitude

$$\delta^n_m = \xi^n e^{imkh}, \quad i = \sqrt{-1}, \tag{29}$$

where k is the mode number and h the element size, is determined from a linearization of the numerical scheme. In order to apply the stability analysis, the Rosenau-KdV equation can be linearized by assuming that the quantity U in the nonlinear term UU_x is locally constant. Substituting the Fourier mode (29) into (23) gives the following equality:

$$\begin{aligned} &\gamma_1\xi^{n+1}e^{i(m-3)kh} + \gamma_2\xi^{n+1}e^{i(m-2)kh} + \gamma_3\xi^{n+1}e^{i(m-1)kh} + \gamma_4\xi^{n+1}e^{imkh} \\ &+ \gamma_5\xi^{n+1}e^{i(m+1)kh} + \gamma_6\xi^{n+1}e^{i(m+2)kh} + \gamma_7\xi^{n+1}e^{i(m+3)kh} = \\ &\gamma_7\xi^{n}e^{i(m-3)kh} + \gamma_6\xi^{n}e^{i(m-2)kh} + \gamma_5\xi^{n}e^{i(m-1)kh} + \gamma_4\xi^{n}e^{imkh} \\ &+ \gamma_3\xi^{n}e^{i(m+1)kh} + \gamma_2\xi^{n}e^{i(m+2)kh} + \gamma_1\xi^{n}e^{i(m+3)kh}. \end{aligned} \tag{30}$$

Now, if Euler's formula,

$$e^{ikh} = \cos(kh) + i\sin(kh), \tag{31}$$

is used in eq. (30) and this equation is simplified, we get the following growth factor:

$$\xi = \frac{\omega - i\varpi}{\omega + i\varpi}, \tag{32}$$

in which

$$\begin{aligned} \omega &= (1208 + 8\mu) + (1191 - 9\mu)\cos(kh) + 120\cos(2kh) + (1 + \mu)\cos(3kh), \\ \varpi &= (245\beta - 19\lambda)\sin(kh) + (56\beta + 8\lambda)\sin(2kh) + (\beta + \lambda)\sin(3kh), \end{aligned} \tag{33}$$

where

$$\beta = E(a + dZ_m), \quad \lambda = M, \quad \mu = K, \quad m = 0, 1, \ldots, N-1. \tag{34}$$

The modulus of $|\xi|$ is 1, therefore the linearized scheme is unconditionally stable.

5 Numerical simulations

Numerical results of the Rosenau-KdV equation are obtained for five test problems: the motion of single solitary wave, interaction of two and three solitary waves, evolution of solitons with Gaussian and undular bore initial conditions. We use the error norm L_2

$$L_2 = \left\|U^{\text{exact}} - U_N\right\|_2 \simeq \sqrt{h\sum_{j=1}^{N}\left|U_j^{\text{exact}} - (U_N)_j\right|^2}, \tag{35}$$

and the error norm L_∞

$$L_\infty = \left\|U^{\text{exact}} - U_N\right\|_\infty \simeq \max_j\left|U_j^{\text{exact}} - (U_N)_j\right|, \quad j = 1, 2, \ldots, N-1, \tag{36}$$

to calculate the difference between analytical and numerical solutions at some specified times. The two conserved quantities that eq. (1) possess are given by [15]

$$I_M = \int_a^b U\,\mathrm{d}x \simeq h\sum_{j=1}^{N} U_j^n, \qquad I_E = \int_a^b [U^2 + c(U_{xx})^2]\mathrm{d}x \simeq h\sum_{j=1}^{N}[(U_j^n)^2 + c\,(U_{xx})_j^n], \tag{37}$$

which represent the momentum and energy of the shallow water waves, respectively. In the simulation of solitary wave motion, the invariants I_M and I_E are monitored to check the accuracy of the numerical algorithm.

5.1 The motion of single solitary wave

The single solitary wave solution of the Rosenau-KdV eq. (1) is given by considered with the boundary conditions $U \to 0$ as $x \to \pm\infty$

$$U(x,t) = A\,\mathrm{sech}^4\left[B\,(x - vt)\right], \tag{38}$$

where

$$A = \frac{210bB^2}{13d}, \quad B = \frac{1}{3}\left[\frac{-13ac + \sqrt{169a^2c^2 + 144b^2c}}{32bc}\right]^{\frac{1}{2}}, \quad v = \frac{b}{52cB^2}. \tag{39}$$

Also, a, b, c and d are arbitrary constants [17]. The initial condition is

$$U(x,0) = A\,\mathrm{sech}^4(Bx). \tag{40}$$

Firstly, to show motion of the single solitary wave numerically, parameters are chosen as $a = 1$, $b = 1$, $c = 1$, $d = 0.5$, $v = 1.18$ and $x\ \epsilon\ [-70, 100]$ for different values of space step (h) and time step (Δt). For these parameters, the single soliton has *amplitude* $= 0.52632$ and the run of the algorithm is carried up to time $t = 40$. The conserved quantities I_M and I_E are tabulated in table 2 together with earlier results. It can be seen from table 2 that the conserved quantities are nearly unchanged as the time processes. It is observed from table 2 that percentage of relative changes of I_M and I_E are found to be $2.221 \times 10^{-6}\%$ and $6.000 \times 10^{-10}\%$ for $h = \Delta t = 0.1$; $9.171 \times 10^{-7}\%$ and $1.400 \times 10^{-9}\%$ for $h = \Delta t = 0.05$; $3.838 \times 10^{-6}\%$ and $3.700 \times 10^{-7}\%$ for $h = \Delta t = 0.05$, respectively. The error norms L_2 and L_∞ are found to be small enough and table 3 represents a comparison of the values of the obtained error norms with earlier results. As seen from table 2 and table 3, the obtained numerical results are better than the earlier results. The motion of the solitary wave is plotted at selected times from $t = 0$ to $t = 40$, in fig. 1. It is observed that the soliton moves to the right at a constant speed and preserves its amplitude and shape with an increasing of time, as expected. The disturbations of the errors at time $t = 40$ are illustrated for single solitary wave in fig. 2.

5.2 Interaction of two solitary waves

Secondly, the interaction of two solitary waves is considered by using the initial condition given by the linear sum of two well-separated solitary waves having different amplitudes

$$U(x,0) = \sum_{i=1}^{2} A_i\,\mathrm{sech}^4\left[B_i\,(x - x_i)\right], \tag{41}$$

where $A_i = \frac{210bB_i^2}{13d}$, $B_i = \left|\sqrt{\frac{b}{52cv_i}}\right|$, $i = 1, 2$, v_i and x_i are arbitrary constants.

Table 2. Comparison of invariants for single solitary wave with $a = 1$, $b = 1$, $c = 1$, $d = 0.5$, $v = 1.18$ and $-70 \leq x \leq 100$ for different values of h and Δt.

$h = \Delta t = 0.1$	I_M			I_E		
t	Present	CLDS [18]	CFEM [21]	Present	CLDS [18]	CFEM [21]
0	5.4981750556	5.4977225480	5.4981750556	1.9897841614	1.9845533653	1.9897841615
10	5.4981749939	5.4977249365	5.4981750556	1.9897841614	1.9845950759	1.9897841624
20	5.4981749598	5.4977287449	5.4981750556	1.9897841614	1.9846459641	1.9897841629
30	5.4981749423	5.4977319638	5.4981750555	1.9897841614	1.9846798272	1.9897841633
40	5.4981749335	5.4977342352	5.4981750621	1.9897841614	1.9847015013	1.9897841635
$h = \Delta t = 0.05$	I_M			I_E		
t	Present	CLDS [18]	CFEM [21]	Present	CLDS [18]	CFEM [21]
0	5.4981692134	5.4980606845	5.4981692134	1.9897831853	1.9843901753	1.9897831853
10	5.4981691962	5.4980608372	5.4981692136	1.9897831854	1.9844010295	1.9897831855
20	5.4981691829	5.4980610805	5.4981692136	1.9897831852	1.9844143675	1.9897831855
30	5.4981691736	5.4980612870	5.4981692134	1.9897831856	1.9844232703	1.9897831854
40	5.4981691629	5.4980613985	5.4981692116	1.9897831853	1.9844289740	1.9897831852
$h = \Delta t = 0.025$	I_M			I_E		
t	Present	CLDS [18]	CFEM [21]	Present	CLDS [18]	CFEM [21]
0	5.4981698357	5.4981454184	5.4981698357	1.9897809061	1.9849493353	1.9897809062
10	5.4981697751	5.4981454791	5.4981698365	1.9897809063	1.9843521098	1.9897809077
20	5.4981697199	5.4981455454	5.4981698322	1.9897809028	1.9843555206	1.9897809038
30	5.4981696708	5.4981456095	5.4981698290	1.9897808998	1.9843578113	1.9897809019
40	5.4981696247	5.4981456591	5.4981698203	1.9897808987	1.9843592922	1.9897808975

Table 3. Comparison of error norms for single solitary wave with $a = 1$, $b = 1$, $c = 1$, $d = 0.5$, $v = 1.18$ and $-70 \leq x \leq 100$ for different values of h and Δt.

$h = \Delta t = 0.1$	$L_2 \times 10^3$			$L_\infty \times 10^3$		
t	Present	CLDS [18]	CFEM [21]	Present	CLDS [18]	CFEM [21]
0	0.000000	0.000000	0.000000	0.000000	0.000000	0.000000
10	0.356724	1.641934	0.370348	0.141639	0.631419	0.149073
20	0.646705	3.045414	0.665684	0.244374	1.131442	0.253418
30	0.902514	4.241827	0.924741	0.326169	1.533771	0.336342
40	1.162489	5.297873	1.187411	0.411492	1.878952	0.422656
$h = \Delta t = 0.05$	$L_2 \times 10^4$			$L_\infty \times 10^4$		
t	Present	CLDS [18]	CFEM [21]	Present	CLDS [18]	CFEM [21]
0	0.000000	0.000000	0.000000	0.000000	0.000000	0.000000
10	0.854386	4.113510	0.888297	0.343706	1.582641	0.362314
20	1.779040	7.631169	1.823510	0.627075	2.835874	0.649564
30	2.810186	10.62971	2.862236	0.975412	3.843906	1.000742
40	3.783328	13.27645	3.842086	1.293116	4.709118	1.320897
$h = \Delta t = 0.025$	$L_2 \times 10^4$			$L_\infty \times 10^5$		
t	Present	CLDS [18]	CFEM [21]	Present	CLDS [18]	CFEM [21]
0	0.000000	0.000000	0.000000	0.000000	0.000000	0.000000
10	0.351702	1.028173	0.357060	1.420544	3.965867	1.421479
20	0.916735	1.905450	0.925408	3.258903	7.097948	3.264848
30	1.043479	2.650990	1.057023	4.681364	9.610332	4.742297
40	1.183139	3.306738	1.183710	4.847163	11.76011	4.846861

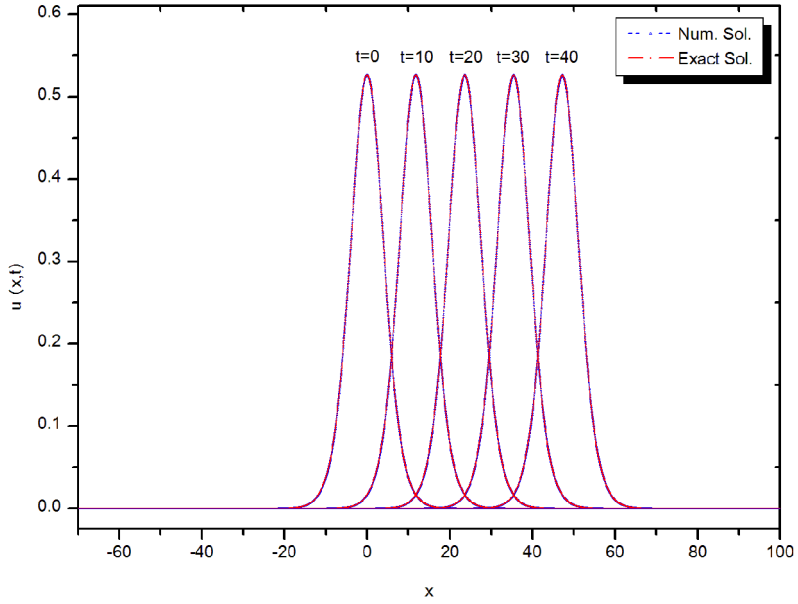

Fig. 1. Motion of single solitary wave with $a = 1$, $b = 1$, $c = 1$, $d = 0.5$, $v = 1.18$, $h = \Delta t = 0.025$ for $-70 \leq x \leq 100$.

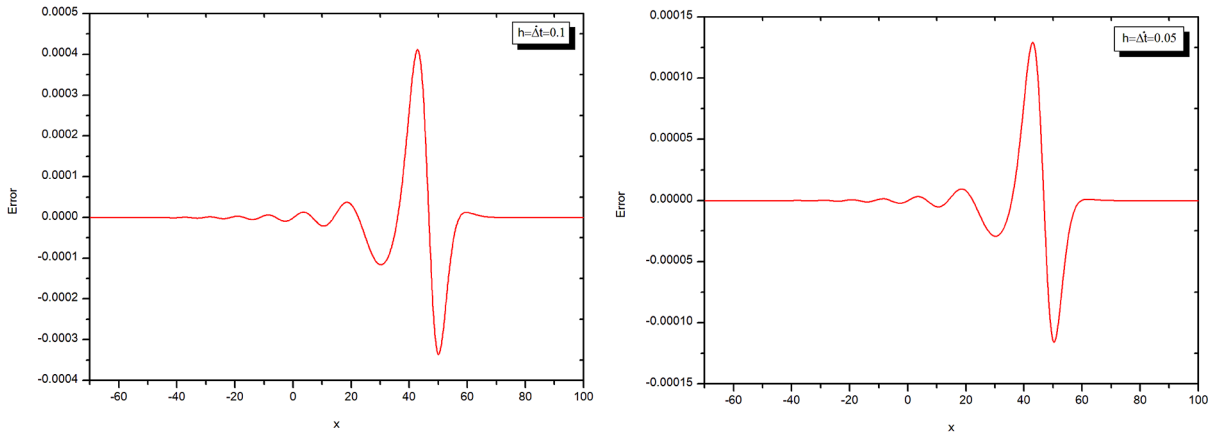

Fig. 2. Error with $a = 1$, $b = 1$, $c = 1$, $d = 0.5$, $v = 1.18$ and $-70 \leq x \leq 100$ for different values of h and Δt at $t = 40$.

For the simulation, the parameters are taken to be $a = 1$, $b = 1$, $c = 1$, $d = 0.5$, $h = 0.1$, $\Delta t = 0.1$, $v_1 = 0.3$, $v_2 = 0.5$, $x_1 = -70$ and $x_2 = -35$ over the range $-100 \leq x \leq 400$. The experiment are run from $t = 0$ to $t = 250$ and the calculated values of the conserved quantities I_M and I_E are reported in table 4. It is seen that the obtained values of the invariants remain almost constant during the computer run. Figure 3 shows the development of the interaction of two solitary waves. It is clear from the figure that, at $t = 0$ the greater soliton is at the left position of the smaller soliton, at the begining of the run. With increasing time the greater soliton catches up the smaller one until time $t = 80$, then the smaller soliton is absorbed. The overlapping process continues until $t = 150$, the greater soliton has overtaken the smaller soliton and gets in the process of separation. At time $t = 250$, the interaction is complete and the greater soliton has separated completely.

5.3 Interaction of three solitary waves

Thirdly, the behavior of the interaction of three solitary waves is studied for different amplitudes. So, eq. (1) is considered with initial condition given by the linear sum of three well-separated solitary waves of different amplitudes

$$U(x,0) = \sum_{i=1}^{3} A_i \operatorname{sech}^4 \left[B_i \left(x - x_i\right)\right], \tag{42}$$

where $A_i = \frac{210bB_i^2}{13d}$, $B_i = \left|\sqrt{\frac{b}{52cv_i}}\right|$, $i = 1, 2, 3$, v_i and x_i are arbitrary constants.

Table 4. The conserved quantities for the interaction of two solitary waves with $a = 1$, $b = 1$, $c = 1$, $d = 0.5$, $h = 0.1$, $\Delta t = 0.1$, $v_1 = 0.3$, $v_2 = 0.5$, $x_1 = -70$ and $x_2 = -35$, $-100 \leq x \leq 400$.

t	I_M	I_E
0	19.3547763167	23.4555195111
50	18.6976052814	23.4623857679
100	18.6524580290	23.4627919923
150	18.6849314916	23.4648227878
200	18.6798456059	23.4658462283
250	18.6670839625	23.4662281908

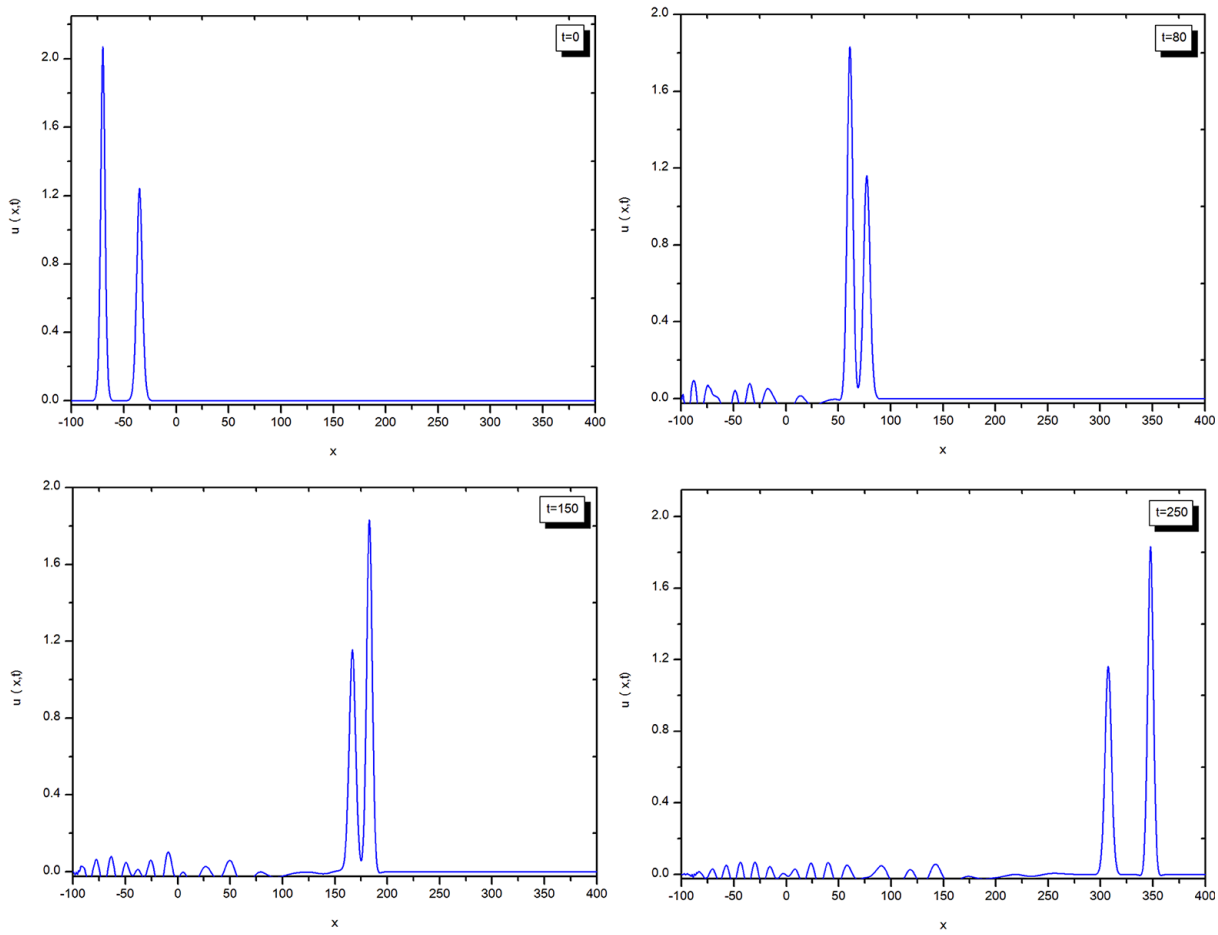

Fig. 3. Interaction of two solitary waves with $a = 1$, $b = 1$, $c = 1$, $d = 0.5$, $h = 0.1$, $\Delta t = 0.1$, $v_1 = 0.3$, $v_2 = 0.5$, $x_1 = -70$, $x_2 = -35$ and $-100 \leq x \leq 400$ at selected times.

For the computational work, parameters $a = 1$, $b = 1$, $c = 1$, $d = 0.5$, $h = 0.1$, $\Delta t = 0.1$, $v_1 = 0.3$, $v_2 = 0.5$, $v_3 = 0.8$, $x_1 = -70$, $x_2 = -40$ and $x_3 = -15$ are taken over the interval $-100 \leq x \leq 400$. Simulations are done up to time $t = 250$. Table 5 displays values of the conserved quantities pending the travelling. It is seen from table 5 that the obtained values of the invariants remain almost constant during the computer run. In fig. 4, the interaction of three solitary waves is depicted. As is seen from fig. 4, interaction started at about time $t = 50$, the overlapping processes occured between time $t = 50$ and $t = 170$ and waves started to resume their original shapes after the time $t = 250$.

Table 5. The conserved quantities for the interaction of three solitary waves with $a = 1$, $b = 1$, $c = 1$, $d = 0.5$, $h = 0.1$, $\Delta t = 0.1$, $v_1 = 0.3$, $v_2 = 0.5$, $v_3 = 0.8$, $x_1 = -70$, $x_2 = -40$ and $x_3 = -15$, $-100 \leq x \leq 400$.

t	I_M	I_E
0	26.0335670001	27.0338255158
50	25.3912010200	27.0410243545
100	25.1890637167	27.0421570504
150	25.1729836835	27.0438944266
200	25.1975503011	27.0448261554
250	25.1823024487	27.0452250712

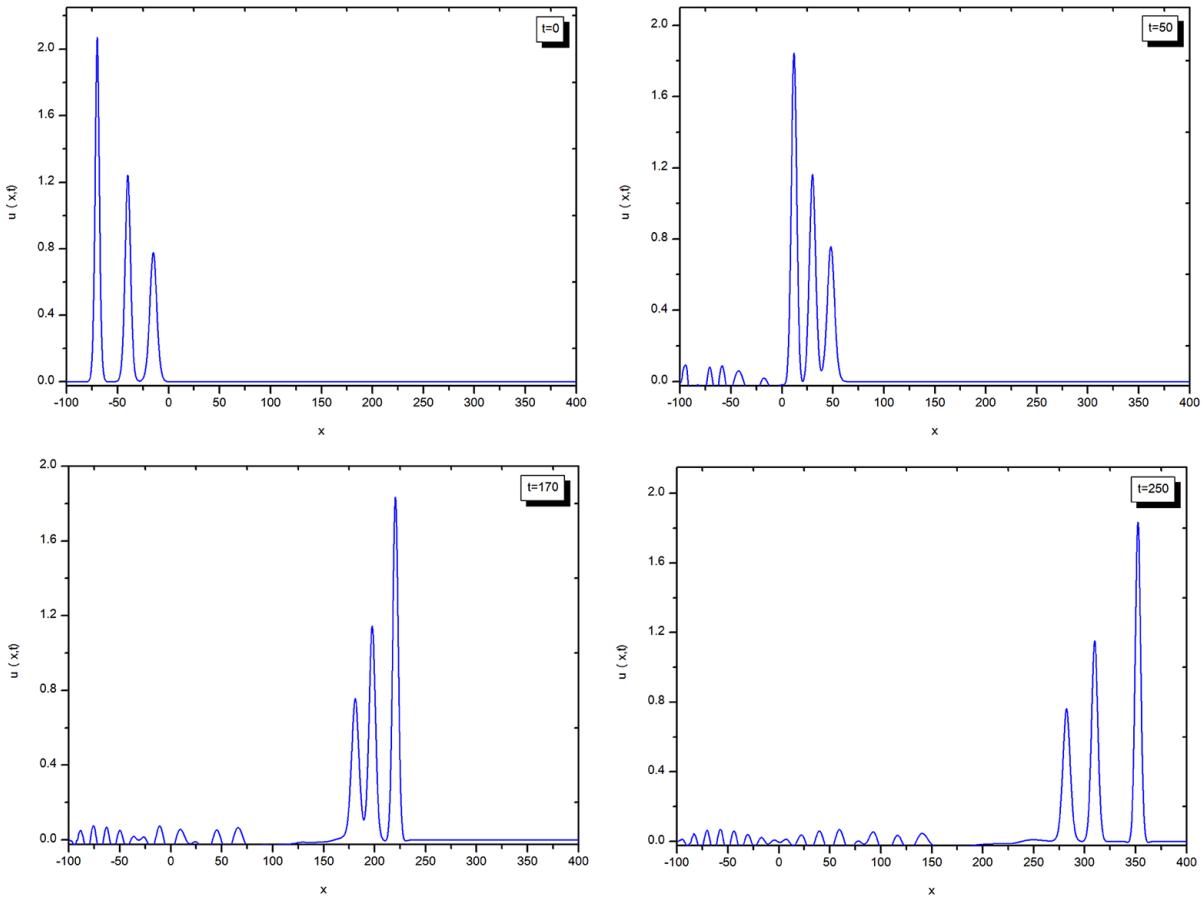

Fig. 4. Interaction of three solitary waves with $a = 1$, $b = 1$, $c = 1$, $d = 0.5$, $h = 0.1$, $\Delta t = 0.1$, $v_1 = 0.3$, $v_2 = 0.5$, $v_3 = 0.8$, $x_1 = -70$, $x_2 = -40$, $x_3 = -15$ and $-100 \leq x \leq 400$ at selected times.

5.4 Evolution of solitons

5.4.1 Gaussian initial condition

Evolution of a train of solitons of the Rosenau-KdV equation is studied using the Gaussian initial condition

$$U(x, 0) = \exp\left[-(x - 40)^2\right], \tag{43}$$

and boundary condition

$$U(-50, t) = U(250, t) = 0, \quad t > 0, \tag{44}$$

Table 6. Invariants for Gaussian initial condition with $a = 1$, $b = 1$, $d = 0.5$, $v = 1.18$, $h = 0.1$, $\Delta t = 0.1$, $-50 \leq x \leq 250$ and different values of c at $0 \leq t \leq 10$.

	$c = 0.5$		$c = 0.1$		$c = 0.05$	
t	I_M	I_E	I_M	I_E	I_M	I_E
0	1.7724808968	3.1332182119	1.7724808968	1.6293102517	1.7724808968	1.4413217567
2	1.7724808968	3.1332186282	1.7724808968	1.6293106040	1.7724808968	1.4413219747
4	1.7724808968	3.1332190741	1.7724808968	1.6293106594	1.7724808968	1.4413219158
6	1.7724808968	3.1332193712	1.7724808968	1.6293106739	1.7724808968	1.4413218732
8	1.7724808968	3.1332196926	1.7724808968	1.6293107034	1.7724808968	1.4413218681
10	1.7724808968	31332197526	1.7724808968	1.6293107402	1.7724808968	1.4413218931

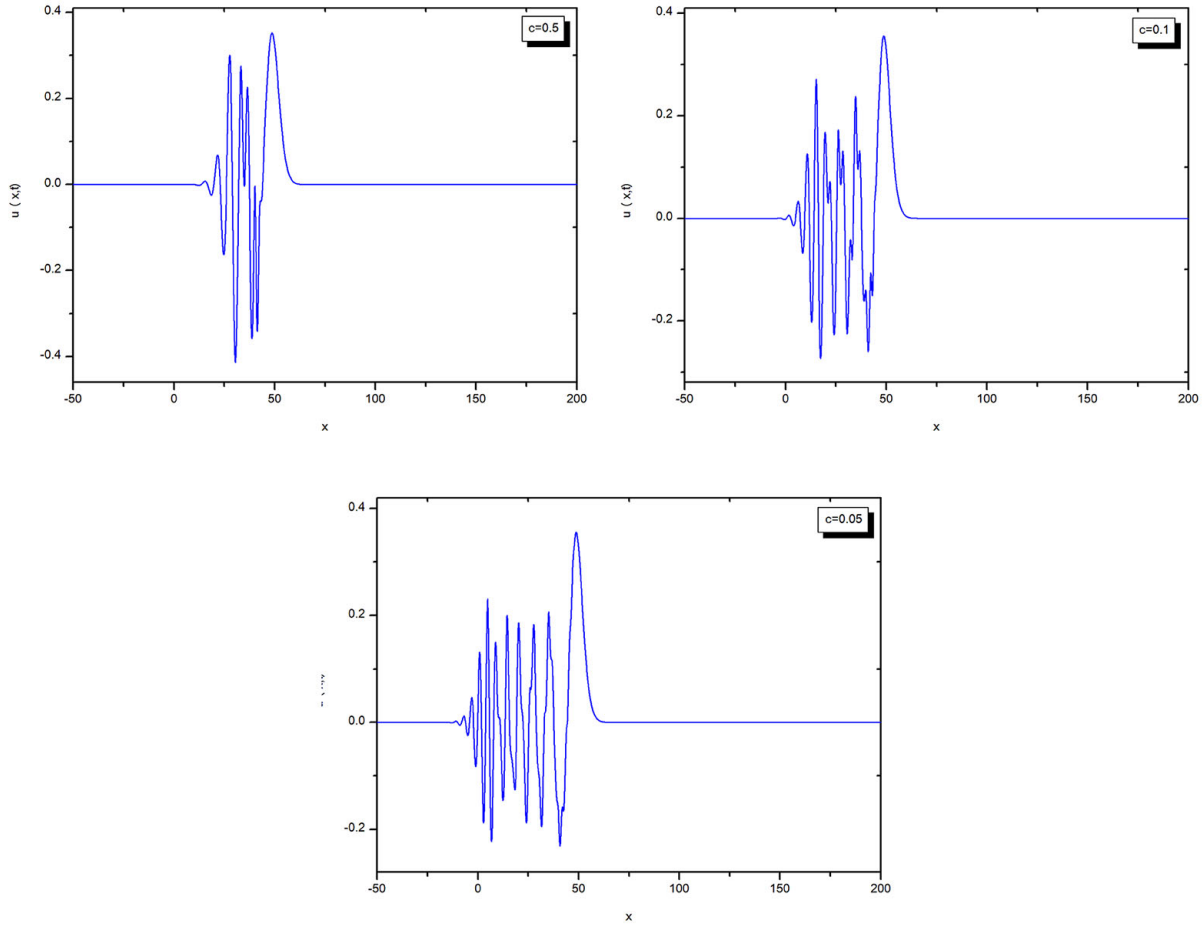

Fig. 5. Generated waves with $a = 1$, $b = 1$, $d = 0.5$, $v = 1.18$, $h = 0.1$, $\Delta t = 0.1$, $-50 \leq x \leq 250$ and different values of c at $t = 10$.

for various values of c. In this case, the behavior of the solution depends on the values of c. Therefore, the values of $c = 0.5$, $c = 0.1$ and $c = 0.05$ are chosen at $0 \leq t \leq 10$.

In this problem, parameters are taken as $a = 1$, $b = 1$, $d = 0.5$, $h = 0.1$ and $\Delta t = 0.1$ over the interval $-50 \leq x \leq 250$. The numerical computations are done up to $t = 10$. The values of the two invariants of motion for different values of c are presented in table 6. The two invariants remain almost constant as the time increases. Also, fig. 5 illustrates the development of the Gaussian initial condition into solitons at $t = 10$.

Table 7. Invariants for undular bore initial condition with $a = 1$, $b = 1$, $c = 1$, $d = 0.5$, $v = 1.18$, $h = 0.1$, $\Delta t = 0.1$ and $-50 \leq x \leq 350$ at $0 \leq t \leq 150$.

t	I_M	I_E
0.0	50.0000031022	45.0046240676
25	49.9962032980	45.0046392765
50	49.9953438219	45.0046467879
75	49.9926519881	45.0046494681
100	49.9947407323	45.0046572374
125	49.9933952569	45.0046645828
150	49.9916251623	45.0046688213

Consequently, oscillating solitons are observed depending on the value of c. Thus, if the value of c is decreased then the number of oscillating solitons increase.

5.4.2 Undular bore initial condition

Finally, evolution of a train of solitons of the Rosenau-KdV equation is worked using the undular bore initial condition

$$U(x,0) = \frac{1}{2}U_0 \left[1 - \tanh\left(\frac{|x| - x_0}{d}\right)\right], \tag{45}$$

and boundary condition

$$U(-50,t) = U(350,t) = 0, \quad t > 0, \tag{46}$$

cause to produce a train of solitons depending upon the value c for Rosenau-KdV equation. The undular bore reflects the elevation of the water above the equilibrium surface at time $t = 0$. The change in water level of magnitude eq. (1) is centered on $x = x_0$ and d measures the steepness of the change. The smaller the value of d the steeper is the slope.

Parameters are taken as $a = 1$, $b = 1$, $c = 1$, $d = 0.5$, $v = 1.18$, $h = 0.1$, $\Delta t = 0.1$, $U_0 = 1$, $x_0 = 25$ and $d = 5$. The program is run up to time $t = 150$. The computed two conserved quantities are listed in table 7. It is seen from the table that the values of the invariants are conserved. Figure 6 shows that the initial perturbation evolves into a well developed train of solitons at selected times. As the time progresses, six solitons moving to the right are observed.

6 Conclusion

In this paper, numerical solution of the Rosenau-KdV equation has been obtained by using subdomain finite element method based on sextic B-spline functions. The presented method has been shown to be unconditionally stable. In addition to the motion of the single solitary wave, the interaction of two and three solitary waves having the different amplitudes which progress in the same direction and the evolution of a train of solitons with Gaussian and undular bore initial conditions have been studied numerically for the first time. These problems that will throw light on the future studies have been supported with simulations visually. The obtained numerical results for single solitary wave show that the adopted method is more accurate than the previously presented results. The study highlights the power of the used method for the determination of numerical solutions to nonlinear evolution equations having wide applications in physical problems modeled by the Rosenau-KdV equation.

The author, Turgut Ak, is grateful to The Scientific and Technological Research Council of Turkey for granting scholarship for Ph.D. studies.

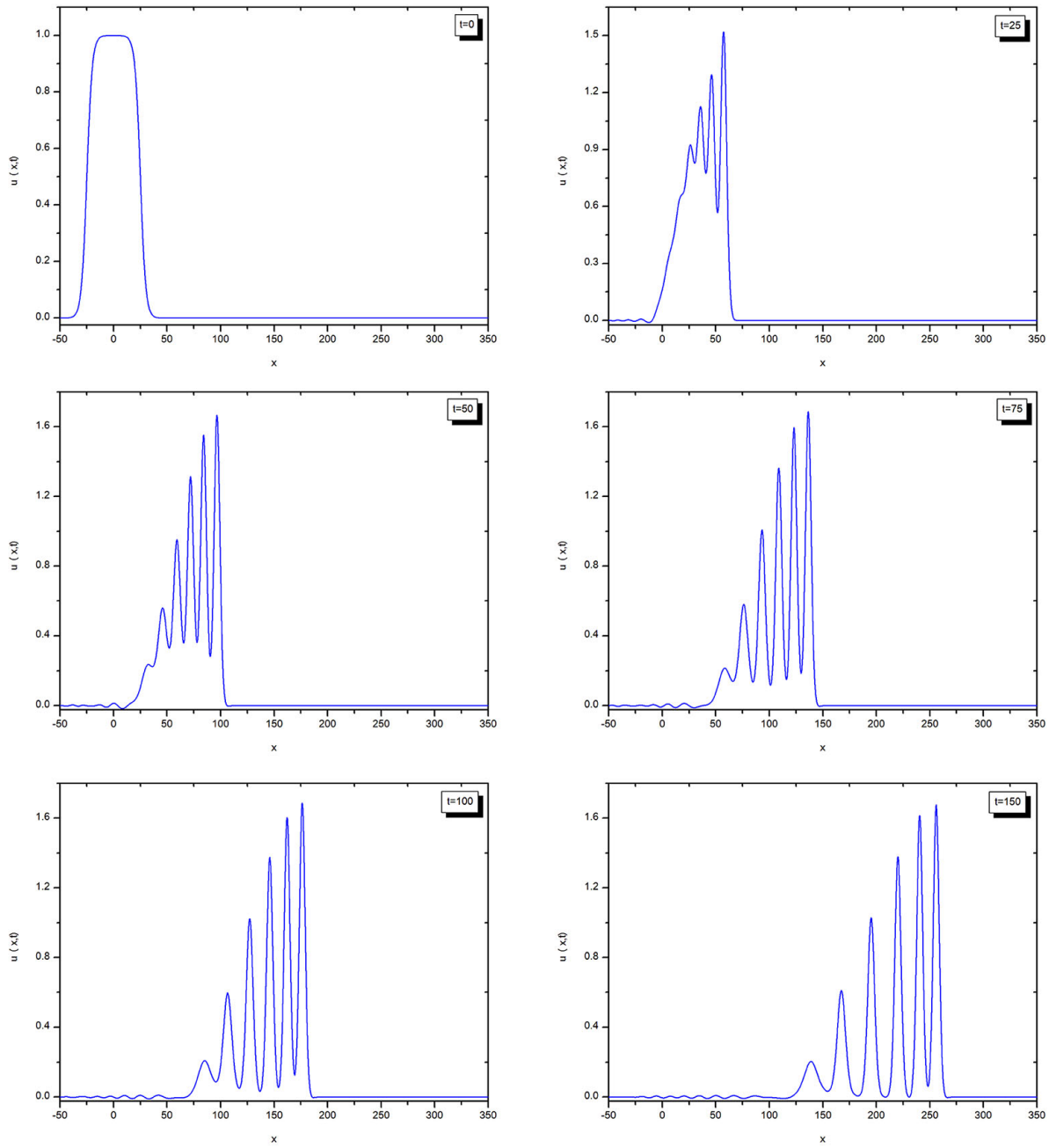

Fig. 6. Developed train of solitons with $a = 1$, $b = 1$, $c = 1$, $d = 0.5$, $v = 1.18$, $h = 0.1$, $\Delta t = 0.1$ and $-50 \leq x \leq 350$ at selected times.

References

1. M.S. Ismail, Appl. Math. Comput. **202**, 520 (2008).
2. M. Dehghan, A. Shokri, Math. Comput. Simulat. **79**, 700 (2008).
3. X. Li, M. Wang, Phys. Lett. A **361**, 115 (2007).
4. H. Triki, A.-M. Wazwaz, Appl. Math. Comput. **214**, 370 (2009).
5. H. Triki, T.R. Taha, Chaos Solitons Fractals **42**, 1068 (2009).
6. K. Nakkeeran, Phys. Rev. E **64**, 046611 (2001).
7. A. Biswas, Phys. Lett. A **372**, 4601 (2008).
8. H. Triki, A.-M. Wazwaz, Phys. Lett. A **373**, 2162 (2009).
9. S. Zhang, Phys. Lett. A **365**, 448 (2007).
10. Z. Feng, Nonlinearity **20**, 343 (2007).

11. T.R. Marchant, Phys. Rev. E **66**, 046623 (2002).
12. T.R. Marchant, Chaos Solitons Fractals **22**, 261 (2004).
13. P. Rosenau, Prog. Theor. Phys. **79**, 1028 (1988).
14. J.-M. Zuo, Appl. Math. Comput. **215**, 835 (2009).
15. A. Esfahani, Commun. Theor. Phys. **55**, 396 (2011).
16. A. Saha, Fund. J. Math. Phys. **2**, 19 (2012).
17. P. Razborova, H. Triki, A. Biswas, Ocean Eng. **63**, 1 (2013).
18. J. Hu, Y. Xu, B. Hu, Adv. Math. Phys. **2013**, 423718 (2013).
19. B. Wongsaijai, K. Poochinapan, Appl. Math. Comput. **245**, 289 (2014).
20. M. Zheng, J. Zhou, J. Appl. Math. **2014**, 202793 (2014).
21. S.B.G. Karakoc, T. Ak, Int. J. Adv. Appl. Math. Mech. **3**, 32 (2016).
22. P.M. Prenter, *Splines and Variational Methods* (John Wiley, New York, 1975) pp. 1–487.